Distribution Agreement

In presenting this thesis or dissertation as a partial fulfillment of the requirements for an advanced degree from Emory University, I hereby grant to Emory University and its agents the non-exclusive license to archive, make accessible, and display my thesis or dissertation in whole or in part in all forms of media, now or hereafter known, including display on the world wide web. I understand that I may select some access restrictions as part of the online submission of this thesis or dissertation. I retain all ownership rights to the copyright of the thesis or dissertation. I also retain the right to use in future works (such as articles or books) all or part of this thesis or dissertation.

Signature:

_____ _____

Geraldine Nabiryo Nabeta Date

A Functional Analysis of SAMHD1 in DNA Double-Strand Break Repair

By

Geraldine Nabiryo Nabeta

Master of Science

Graduate Division of Biological and Biomedical Science

Cancer Biology and Translational Oncology

_____

David Yu, M.D., Ph.D.
Advisor

_____

Xingming Deng, M.D., Ph.D.
Committee Member

_____

William Dynan, Ph.D.
Committee Member

_____

Baek Kim, Ph.D.
Committee Member

Accepted:

_____

Lisa A. Tedesco, Ph.D.
Dean of the James T. Laney School of Graduate Studies

_____

Date

A Functional Analysis of SAMHD1 in DNA Double-Strand Break Repair

By

Geraldine Nabiryo Nabeta
B.A. , Emory University, 2016

Advisor:

David Yu, M.D., Ph.D.

An abstract of a thesis submitted to the Faculty of the James T. Laney School of Graduate Studies of Emory University in partial fulfillment of the requirements for the degree of Master of Science in the Graduate Division of Biological and Biomedical Science, Cancer Biology and Translational Oncology, 2017.

Abstract

A Functional Analysis of SAMHD1 in DNA Double Stranded Break Repair

By Geraldine Nabiryo Nabeta

Genomic DNA is subject to exogenous or endogenous damage, which results in insults to the DNA as either single-strand or double-strand lesions. DNA double-strand breaks (DSBs) are predominantly repaired by two mechanisms, the homologous recombination(HR) and non-homologous end joining (NHEJ). The mechanism homologous recombination is of particular interest. SAMHD1 is a deoxynucleotide triphosphohydrolase (dNTPase) that restricts HIV-1 infection by depleting dNTPs necessary for reverse transcription and replication. SAMHD1 is also a protein assumed to regulate cell proliferation and survival in response to DNA damage. Although the direct mechanism through which SAMHD1 is involved in DNA repair is unclear, our laboratory has demonstrated a novel role in promoting DNA end resection, which facilitates DNA DSB repair via HR. Mutations and dysregulation of SAMHD1 have also been implicated in various cancers, although their functional significance is unknown. Taken together, these findings suggest that SAMHD1 association with cancer could be due to its role in the DNA DSB repair response, which is required to maintain genome integrity. For the following project, disease-relevant SAMHD1 mutations (DRSM) – D137N and K484T - reveal SAMHD1's role in double-strand break repair. I hypothesize that disease relevant mutations may affect SAMHD1's contribution in DNA end resection. This report serves as a preliminary functional analysis of SAMHD1 mutants.

A Functional Analysis of SAMHD1 in DNA Double-Strand Break Repair

By

Geraldine Nabiryo Nabeta
B.A., Emory University, 2016

Advisor:

David Yu M.D., Ph.D.

A thesis submitted to the Faculty of the James T. Laney School of Graduate Studies of Emory University in partial fulfillment of the requirements for the degree of Master of Science in the Graduate Division of Biological and Biomedical Science, Cancer Biology and Translational Oncology, 2017.

ACKNOWLEDGEMENTS

First, I would like to thank my thesis advisor David Yu M.D., Ph.D. . His office was always open to me whenever I had a myriad of questions about my research. He guided my work, yet consistently allowed this project to be my own work.

I would also like to thank my committee members for contributing their expertise, time and valuable input: William Dynan Ph.D., Xingming Deng M.D. Ph.D., and Baek Kim Ph.D. .

I would like to acknowledge the members of the Yu laboratory for all the teaching, constant encouragement and commitment to my training. I would like to thank Waaqo Daddacha Ph.D., in particular, for his guidance and mentorship, which have been instrumental in both the making of this thesis and my growth as a scholar.

Finally, I wish to express my most sincere gratitude to my parents, my siblings, extended family and friends for wholeheartedly believing in my potential, and for providing me with unfailing love and support. This accomplishment would not have been possible without them.

I am gratefully indebted to everyone who played a part (big or small) in the making of this thesis.

Geraldine Nabiryo Nabeta

Table of Contents

Table of Figures

List of Abbreviations

DSB	Double-Strand Break
HR	Homologous recombination
NHEJ	Non-homologous end joining
PTM	Post-translational modification
DRSM	Disease-relevant SAMHD1 mutations
ssDNA	single-stranded DNA
BrdU	5-bromo-2'-deoxyuridine
DMEM	Dulbecco's Modified Eagle Medium
DR GFP	Direct repeat GFP
dNTP	Deoxynucleotide triphosphates
WT	Wild type
NS	Nonspecific

INTRODUCTION

An Overview of DNA Double Stranded Break Repair

Our DNA is the blueprint for our body. It contains the genetic instructions for the function and development of all living cells. Cells also possess mechanisms that act in response to diverse stressors, such as DNA damage. Our DNA is constantly exposed to damage from agents in our environment or within the microenvironment of our bodies. For instance, human DNA commonly experiences damage from UV rays emitted from the sun and from byproducts of metabolic processes.

As genomic DNA is subjected to exogenous or endogenous damage, a variety of insults are imposed on our DNA, including single-strand or double-strand breaks. I will focus here on double-strand lesions breaks (DSB), which are predominantly repaired via two mechanisms, homologous recombination (HR) and non-homologous end joining (NHEJ) (Figure 1) *[1]*.

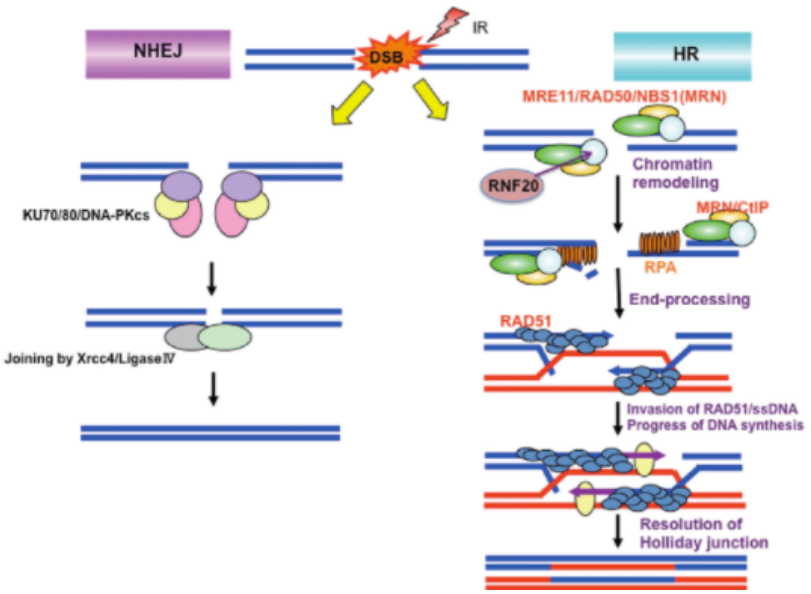

Siato et. al, 2013

***Figure 1**: Non-homologous end joining and homologous recombination, and their participating proteins.*

NHEJ is characterized by the direct ligation of DNA ends, and is an error-prone pathway. HR uses a sister chromatid as a template to repair DNA, and is the less error prone. These pathways also differ in their prevalence in different cell cycle phases. NHEJ repair is occurs throughout the cell cycle, whereas HR prevails in the S and G2 phases. The balance in expression between critical proteins, 53BP1 and BRCA1, helps determine the cell's repair pathway preference (Figure 2).

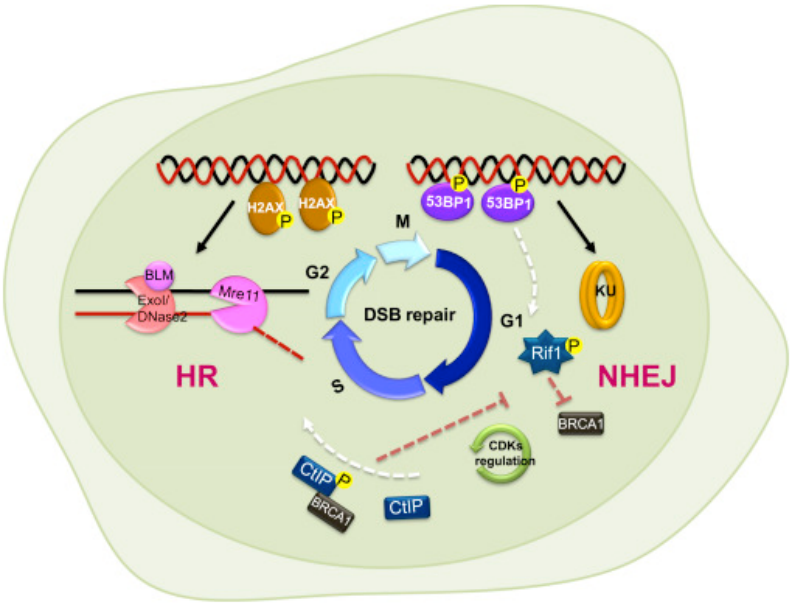

Srivastava et. al, 2015

Figure 2: Factors in the choice between DNA double-strand break repair pathways

The choice between DNA double-strand break repair pathways, NHEJ, and HR, is determined by various regulatory mechanisms. HR is predominant in S and G2 phases of the cell cycle, whereas NHEJ is active throughout the cell cycle, playing a major role during G1 and M phases. Negative regulation of BRCA1 by 53BP1 commits the cells repair to either HR or NHEJ. The phosphorylation of CtIP throughout the S phase and the complex formation with BRCA1 facilitates HR repair. Regulators within this pathway can serve as potential therapeutic targets.

53BP1 act as an inhibitor of BRCA1 and vice versa; 53BP1 acts to inhibit the association of BRCA1 with downstream end resection protein complexes, like MRN [2] Therefore, as the cell enters the G1 phase its expression of 53BP1 increases and inhibits BRCA1, thus directing the cell to favor NHEJ repair upon the induction of double strand lesions. As the cell proceeds into the S and G2 phases of the cell cycle its expression of BRCA1 is elevated, thus favoring the HR pathway for DSB repair, and inhibiting 53BP1 through unknown mechanisms [2]. The HR pathway involves a series of interactions between components of the pathway. HR is initiated by the recruitment of the CtIP/MRN complex to sites of DSB. This complex resects the DNA and exposes a 3' single-stranded DNA (ssDNA) overhang. Following this, is the later part of end resection, known as extensive resection, which is carried out by EXO1 and DNA2. Upon DNA end resection, the 3' ssDNA overhangs are coated with RPA in order to prevent secondary structure formation in the single-stranded region [3]. Although DSB repair pathways have been thoroughly investigated, the precise mechanisms and proteins upon which they are dependent are not fully understood. DSB repair proteins determine cancer treatment responses. Thus an understanding of novel DSB repair proteins provides insightful therapeutic approaches to developing novel targets and treatment [4] As discussed in the next section, one of the targets may be SAMHD1.

.

SAMHD1

Human SAMHD1 is composed of 626 amino acids, and exists in tetramer and monomer/dimer forms (Figure 3). In the tetramer SAMHD1 has deoxynucleotide triphosphohydrolase (dNTPase) activity and the monomer/dimer may have nuclease activity [5].

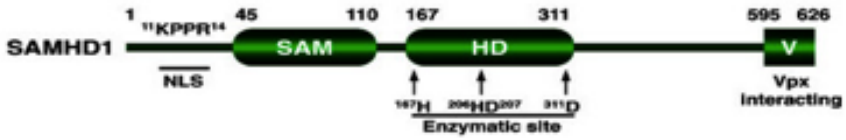

Zheng et. al 2012

***Figure 3**: **SAMHD1 Domains.** A nuclear localization sequence (NLS) KRPR resides near the N-terminus, a SAM domain between residues 45–110, an HD domain between residues 167–311, and a variable domain, commonly a Vpx site for degradation purposes near the C-terminus.* [6].

SAMHD1 oligomerizes through its HD domain, and this is required for its triphosphohydrolase activity [7] As a dNTPase SAMHD1, converts deoxynucleotide triphosphates to their deoxynucleoside and inorganic triphosphate constituents [8]. There are conflicting reports whether SAMHD1 has intrinsic nuclease activity and whether this is involved in HIV restriction [9] [10] [11]. A recent report described a phosphorolytic

ribonuclease activity associated with SAMHD1, which is only observed in the presence of free inorganic phosphates. This may explain earlier differing observations.

The Clinical Relevance of SAMHD1

The role of SAMHD1 is most extensively studied within viral infections, but most notably in HIV-1 as a factors that limits reverse transcription and restricts viral infection (Figure 4).

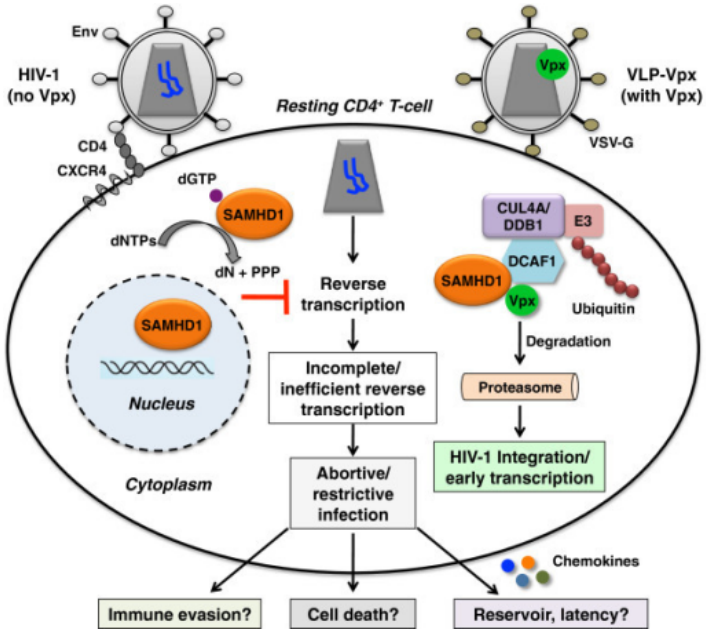

Figure 4. SAMHD1 restricts HIV-1 infection in resting CD4+T-cells by limiting viral reverse transcription. *SAMHD1 is a dNTP triphosphohydrolase that converts intracellular dNTPs to its constituent deoxynucleosides (dN) and inorganic triphosphate (PPP), thereby resulting in inefficient HIV-1 reverse transcription in CD4+ T-cells. Conversely, HIV-2 expresses Vpx which degrades SAMHD1. The treatment of resting CD4+ T-cells with Vpx expression results in proteasomal degradation of SAMHD1 and leads to HIV-1 integration and early transcription of the gene [12]*

SAMHD1's ability to regulate dNTP levels challenge the viral replication mechanisms to function appropriately and promote disease progression. Interestingly, the role of SAMHD1 was first discovered in Aicardi- Goutieres Syndrome (AGS), whereby SAMHD1 mutations were implicated in patients with AGS. AGS is a rare autoimmune disease inherited in an autosomal recessive manner. With an early childhood onset, AGS is generally fatal and results in a persistent vegetative state [13]. As the disease progresses, patients experience a wide range of neurodegenerative and physically impairing symptoms. Encephalopathy, dystonia, and skin lesions, are especially common. AGS is frequently diagnosed using MRI scans and by sampling of the cerebrospinal fluid from a spinal tap, to screen for lymphocytosis. There is no cure for AGS and therefore, current treatment plans revolve around palliative care and experimental treatments.

Germline mutations of SAMHD1 have been observed in patients with both AGS and various cancers. Clifford et. al's 2014 paper, "SAMHD1 is mutated recurrently in chronic lymphocytic leukemia and is involved in response to DNA damage" investigated SAMHD1 mutations and the clinical outcomes in patients. Their study found that 17% of patients diagnosed with AGS possessed germ-line SAMHD1 mutations. They used the case of a 24-year old male with AGS who developed chronic lymphocytic leukemia (CLL) as a framework for their further investigation into SAMHD1 mutations implicated in a clinical setting. Upon further exploration, their findings reported that 11% of relapsed CLL patients acquired pathogenic mutations of SAMHD1. Therefore suggesting that, mutations in SAMHD1 are to be considered as potential founding events for CLL. Their study also

revealed that SAMHD1 mutations implicated in AGS overlapped with mutations observed in CLL, namely R145Q and I201N. These overlapping mutations suggest that SAMHD1 dysregulation is implicated in diseases characterized by genomic instability, and thus have significance in promoting the pathogenesis of AGS and CLL.

Considering that both AGS and CLL are diseases characterized by genomic instability, this makes SAMHD1 a point of interest in its role to maintain genomic integrity. Genomic integrity is commonly maintained through mechanisms that promote stability and replication, such as DNA repair [14] . If errors in either mechanisms accumulate, they expose the cells to genomic instability, and promote the development of chronic diseases such as Cancer. In the case of SAMHD1 depletion of the dNTP pool resulting from dysfunctional SAMHD1 is associated with DNA replication stress [15]. This leads to mutagenesis, genomic instability, and cancer development [16] Therefore, SAMHD1's potential to maintain genome integrity can be studied through is the DNA repair pathway.

SAMHD1 mutations have also been implicated in other cancers. Colon cancers have altered intracellular dNTP pools, based on the observation that SAMHD1degrades dNTPs. The mutations identified in colon cancers decrease SAMHD1's dNTP triphosphohydrolase activity [17], suggesting that this activity contributes to tumor suppression. Figure 5 provides an additional analysis from the Human Protein Atlas of SAMHD1 expression in a variety of cancers. Most strikingly we find the increase in expression from their normal counterparts observed in glioma, carcinoid, breast cancer, liver cancer, skin cancer, stomach cancer, and thyroid cancer.

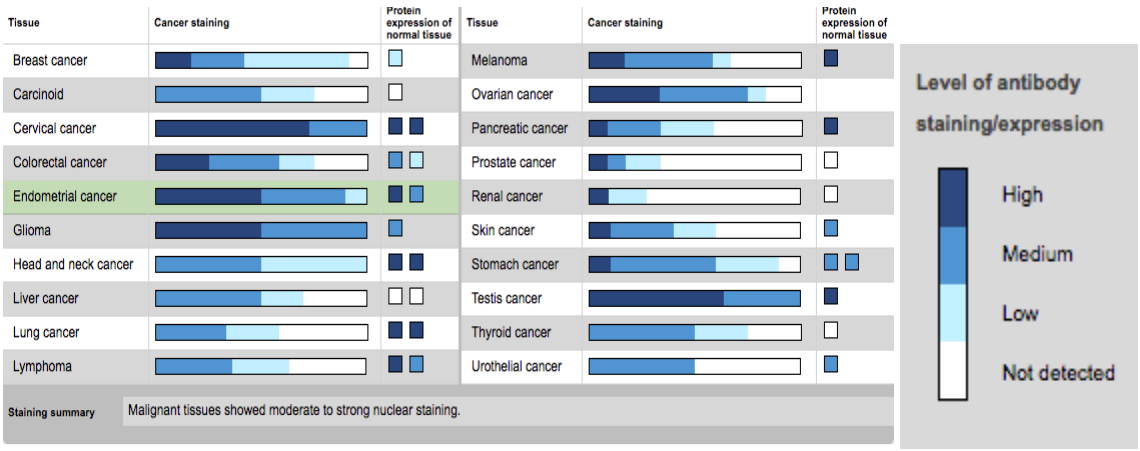

Human Protein Atlas

***Figure 5**: **Expression of SAMHD1 in tumor and normal tissue.** Varying expression of SAMHD1 in cancers listed and their corresponding normal tissue.*

This image is indicative of the presence of SAMHD1 mutations in several human cancer tissue samples [18], thus strengthening the clinical relevance of this protein and the possibility of using SAMHD1 in the quest to developing novel treatments against cancer.

SAMHD1 and DNA Double-Strand Break Repair

Previous work have shown that SAMHD1 localizes to sites of DNA damage. Data from our laboratory, show SAMHD1 colocalizes with the DNA damage marker, γH2AX. (Figure 6).

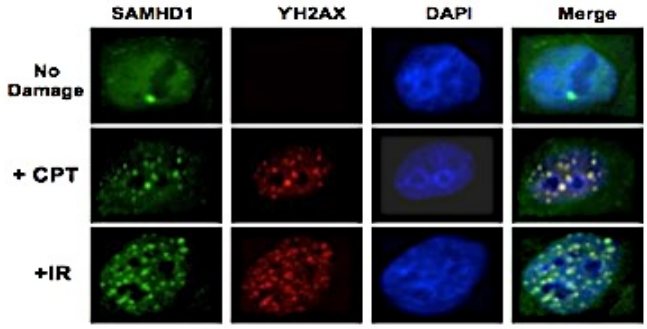

Figure 6: SAMHD1 recruitment to damage sites. *Colocalization of SAMHD1 and γH2AX in U2OS cells under damage conditions: 4 h of 3 μM Camptothecin (CPT) and 10 Gy irradiation with 4 h recovery period. Protein visualization is carried out by immunofluorescence, following 4% PFA fixation.*

Additionally, preliminary data from a Direct Repeat GFP (DR GFP) assay suggests that SAMHD1 is involved in HR (Figure 7). The DR GFP assay uses increases in GFP intensity, measured by flow cytometry, to provide a qualitative and quantitative readout of homologous recombination efficiency (see appendix I.1)

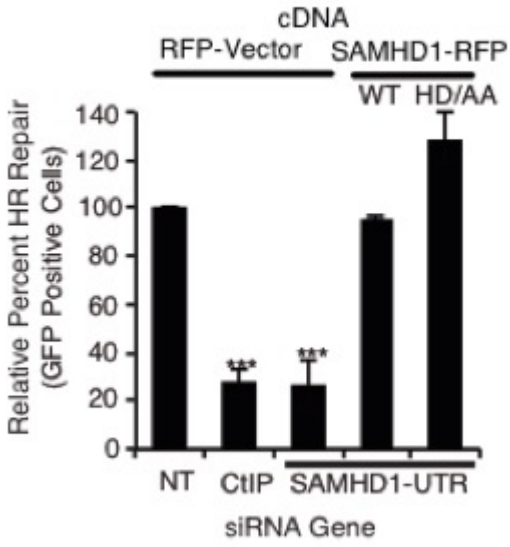

***Figure 7*: Homologous recombination is limited with SAMHD1 depletion.** *U2OS cells contain an I-SceI endonuclease site. Cleavage at this site, followed by HR repair leads to GFP expression. Cells were treated with CtIP siRNA as a positive control, SAMHD1-UTR siRNA, SAMHD1-UTR siRNA and WT or SAMHD1-UTR siRNA HD/AA catalytically dead mutant of SAMHD1.*

This data demonstrates that cells transfected with SAMHD1-UTR siRNA show reduced HR activity. This phenotype is rescued by re-expression of SAMHD1 wild type or mutant (SAMHD1 HD/AA) proteins. One hypothesis is that SAMHD1 is involved in DNA end

resection. Consistent with this, SAMHD1 siRNA treatment of U2OS cells results in a reduction in RPA70 foci, a marker of DNA end resection, localization to laser micro-irradiated DNA damage sites (Figure 8).

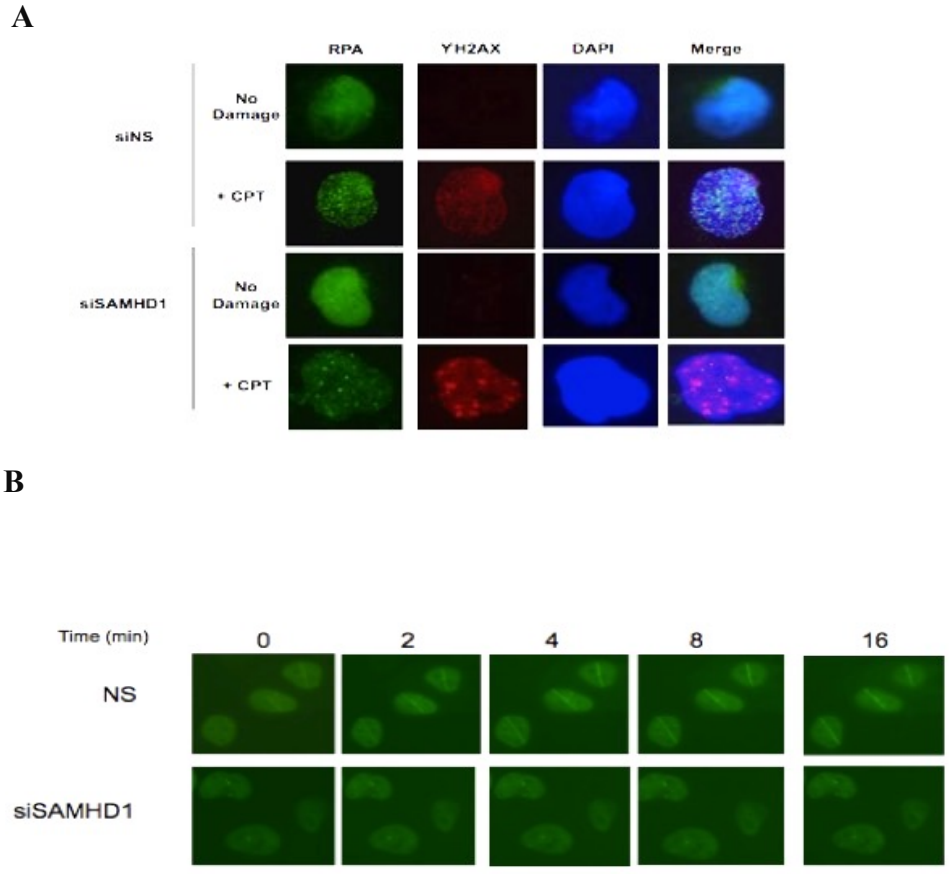

Figure 8: ***SAMHD1 depletion leads to impaired RPA70 recruitment to damage sites as measured by Immunofluorescence and laser microirradiation assay.***

A) U2OS cells treated with SAMHD1 siRNA and siNS under damage conditions:

4 h of 3 μM Camptothecin (CPT) providing an impairment of RPA 70 foci formation in the siSAMHD1 in comparison to the siNS. Protein visualization is carried out by immunofluorescence, incorporating 4% PFA fixation. B) U2OS cells with a SAMHD1 siRNA also show reduced recruitment of RPA 70 to laser induced damage sites (365nm), in comparison to the nonspecific siRNA cells.

These findings support SAMHD1's involvement in homologous recombination by way of DNA end resection. These data from the rationale for my studies, which involve futher functional of SAMHD1 in DNA DSBR. There is evidence that SAMHD1 mutations are associated with several cancers. Our work shows that SAMHD1 is involved in DNA DSB repair via (HR). Taken together, these findings suggest the association of SAMHD1 mutations and dysregulation with cancer could be due to its role in DNA DSB repair and impairment of its potential to maintain genome integrity.

Scope of the Thesis

SAMHD1 exists in both tetramer and monomer/dimer forms. In either conformation SAMHD1 exhibits varying levels of activity. In its tetramer form SAMHD1 has triphosphohydrolase activity (dNTPase), which reduces the availability of intracellular dNTP's for essential DNA replication. As a monomer, SAMHD1 exhibits nuclease activity (Figure 9). Although there has been controversy whether this is intrinsic to SAMHD1, recent results are consistent with a phosphorolytic RNase activity.

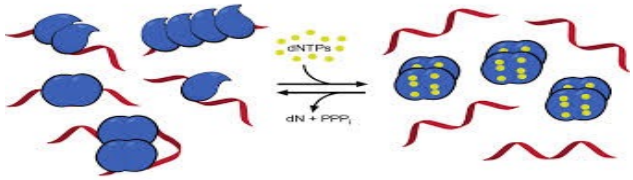

Seamon et. al, 2015

Figure 9: SAMHD1 exists as a tetramer or monomer/dimer. *Equilibrium of SAMHD1 conformations as a tetramer catalyzing dNTP degradation, or as monomer/dimer exhibiting nuclease activity*

Mutations of SAMHD1 are presumed to disrupt either one of its activities [19] . However, there is limited background on SAMHD1 mutations and their implications on SAMHD1 functionality. The significance of this project serves as an initial investigation into the effects of SAMHD1 mutations on SAMHD1 HR activity. Therefore, the following project explores two disease relevant mutations, both of which were identified and chosen for exploration for unique reasons: D137N and K484T.

Reconstructions of SAMHD1 mutations found in cancer, have yet to be biochemically characterized into SAMHD1 expression vector. The D137N mutation affects a dGTP binding site on SAMHD1. The dGTP binding destabilizes the tetramer form of SAMHD1 and is essential for dNTP triphosphohydrolase activity. Loss of dGTP binding activity favors the monomer/dimer form [11].

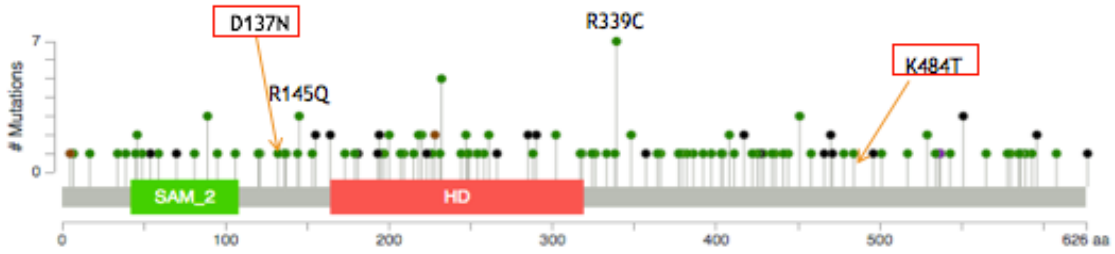

Figure 10: cBioportal analysis of SAMHD1 mutations. *Collection of SAMHD1 mutations observed in patients diagnosed with a diverse range of cancers.*

The other mutation, K484T, though clinically not as impactful (Figure 10), affects a residue that it is a potential target for post-translational modifications. Post-translational modifications (PTM) are common mechanisms for protein regulation. A PTM already explored for SAMHD1 is phosphorylation. The effect of SAMHD1 phosphorylation on activity has been previously studied [20]. Moreover, T592 has been identified as a phosphorylation site [21] , though the significance of T592 phosphorylation in disease is not fully understood. Therefore, it is possible that other PTMs occur in SAMHD1. In the case of K484, lysine (K) is a candidate for PTM by acetylation or ubitiquination. Consistent

with this, is the location of the K484 residue on the surface of SAMHD1 (Figure 20), thus exposing it to acetyl transferases and other post-translational modification enzymes. However, an analysis of mutations at potential PTM sites will clarify how PTM can contribute towards SAMHD1 activity.

Mutational analysis is a useful approach for identifying how vulnerabilities in SAMHD1's function can be considered as potential therapeutic targets in the DNA repair pathway. I hypothesize that disease-relevant SAMHD1 mutations may affect SAMHD1's role in DSB repair, particularly by impairing its role in DNA end resection. To test this hypothesis, I addressed the question: Do the SAMHD1 disease relevant mutations affect its ability to promote DNA DSB repair? As a means to further analyze SAMHD1 role in DNA DSB repair and particularly end resection, I used a BrdU assay and a foci formation assay as indicators of DNA end resection. I tested the ability of SAMHD1 mutants to rescue resection activity in SAMHD1 siRNA treated cells. Preliminary data from our laboratory also shows an interaction between CtIP and SAMHD1 in irradiated cells. In these prior studies the laboratory identified the 115-562 region on SAMHD1 as the CtIP interacting domain. Therefore, I used a co-Immunoprecipitation to illustrate an interaction between CtIP and SAMHD1 mutations. Lastly, in order to further refine the interacting region between CtIP and SAMHD1, I analyzed of a co-Immunoprecipitation between CtIP and SAMHD1 truncations within the 115-562 region: 1-115, 1-165, 1-215, 1-315,1-465, 1-562.

MATERIALS AND METHODS

Site Directed Mutagenesis

Primers (D137N and K484T) for SAMHD1 mutagenesis were designed using SnapGene® software (from GSL Biotech; available at snapgene.com)[22]. Primers were amplified in SAMHD1-GFP [1] and pKH3 (HA) [23] vectors [2] [23]. Following PCR amplification, products were digested with DpnI for 2 h and then transformed into *E. Coli* DH5α. Three colonies from each sample were picked and sequenced according to Macrogen sequencing guidelines. Sequences were analyzed and confirmed using Snapgene software.

5-bromo-2'-deoxyuridine (BrdU) assay

Human U2OS cells were cultured in Dulbecco's Modified Eagle Medium (DMEM) were and transfected with 30 nm of siRNA using Lipofectamine RNAi Max (Invitrogen), following the manufacturer's instructions. The following siRNA were transfected: nonspecific siRNA (ATGAACGTGAATTGCTCAATT), SAMHD1 5' UTR siRNA (ACGCAUGCUGAAGCTAAGTAA) and SAMHD1 #1 siRNA (CAACCAGAGCUGCAGAUAA). Cells were seeded on cover slips and after 24 h, 30 μM 5-bromo-2'-deoxyuridine (BrdU) was added to the medium after a further 36 h.

[1] pcDNA3-EGFP was a gift from Doug Goldenbock Addgene, plasmid #13031
[2] pKH3 was a gift from Ian Macara. Addgene plasmid #12555

Cells were irradiated 10 Gy, allowed to recover 4 h and fixed (see appendix I.7 for protocol). Samples were incubated with anti-BrdU (BD Biosciences, 555627) and anti-γH2AX (Cell Signaling, 2577S) overnight at 4 °C. After secondary antibody staining, images were collecting using a Zeiss confocal microscope.

Co-Immunoprecipitation

Human HEK293 cells were cultured in DMEM and transfected with GFP-CtIP plasmid using Lipofectamine 3000 transfection reagent (Invitrogen) following the manufacturer's protocol. At 24 h post GFP-CtIP transfection, cells were transfected with wild type (SAMHD1-HA WT) or mutant SAMHD1-HA (K484T, D137N, R339C and R145Q) expression constructs. After a further 48 h, cells were irradiated, allowed to recover 4 h and harvested. Cells were lysed on ice with constant agitation in lysis buffer (10% glycerol, 150 mM NaCl, 50 mM Tris pH 7.5, cocktail of protease inhibitors) containing 0.75% CHAPS. Lysates were centrifuged at 4 °C at 13,000 RPM for 15 min. The protein concentration for each sample was measured by a bicinchoninic acid assay. Approximately 2-3mg of protein were used for IP. Samples were pre-cleared with G-Protein agarose beads (Roche Diagnostics, 704746211) at 4 °C overnight. Following the pre-clear, the samples were incubated with anti-HA- conjugated beads (Sigma, A2095) overnight at 4 °C. Immune complexes were eluted and resolved by 5-20% SDS PAGE, proteins were transferred to a PVDF membrane, which was probed with anti-GFP (Genetex, 113617) and anti-HA (Sigma, H9658) at 1:1000 dilutions.

Immunofluorescence protocol

Human U2OS cells transfected with 30 nm of siRNA using Lipofectamine RNAi Max (Invitrogen), following the manufacturer's instructions. The following siRNA were transfected: nonspecific siRNA (ATGAACGTGAATTGCTCAATT) and SAMHD1 5' UTR siRNA (ACGCAUGCUGAAGCTAAGTAA). Cells were seeded on cover slips and after 24 h knockdown transfected with SAMHD1-GFP WT and D137N expression constructs. After a further 48 h, cells were irradiated with 10 Gy IR and allowed to recover for 4 h of recovery. They were fixed with 4% PFA and permeabilized with 0.5% Triton X-100. Immunodetection was achieved through incubating samples in polyclonal anti-RPA70 (Cell signaling #2267) and anti-γH2AX (Cell Signaling, 2577S) overnight. After secondary antibody staining, images were collecting using a Zeiss confocal microscope.

RESULTS

BrdU as a marker for End Resection

In the experiment showing in Figure 11, I used BrdU foci assay as a marker for DNA end resection. The purpose in using this assay was to provide initial confirmation that SAMHD1 is required for efficient end resection. BrdU is a thymidine analog, that is incorporated into the DNA during replication. Anti-BrdU recognizes BrdU in the context of single-stranded but not double-stranded DNA. When ssDNA is revealed during DNA end resection following the induction of double stranded lesions, BrdU sites of incorporation are exposed. Figure 11.A demonstrates that untreated cells have RPA70 foci coinciding with γH2AX. Cells treated with either siRNA (siSAMHD1 #1 or siSAMHD1 UTR) depleting SAMHD1, show a decrease in RPA70 foci coinciding with γH2AX. This finding is indicative of a reduction in end resection efficiency, potentially due to SAMHD1 depletion impairing RPA70 foci formation.

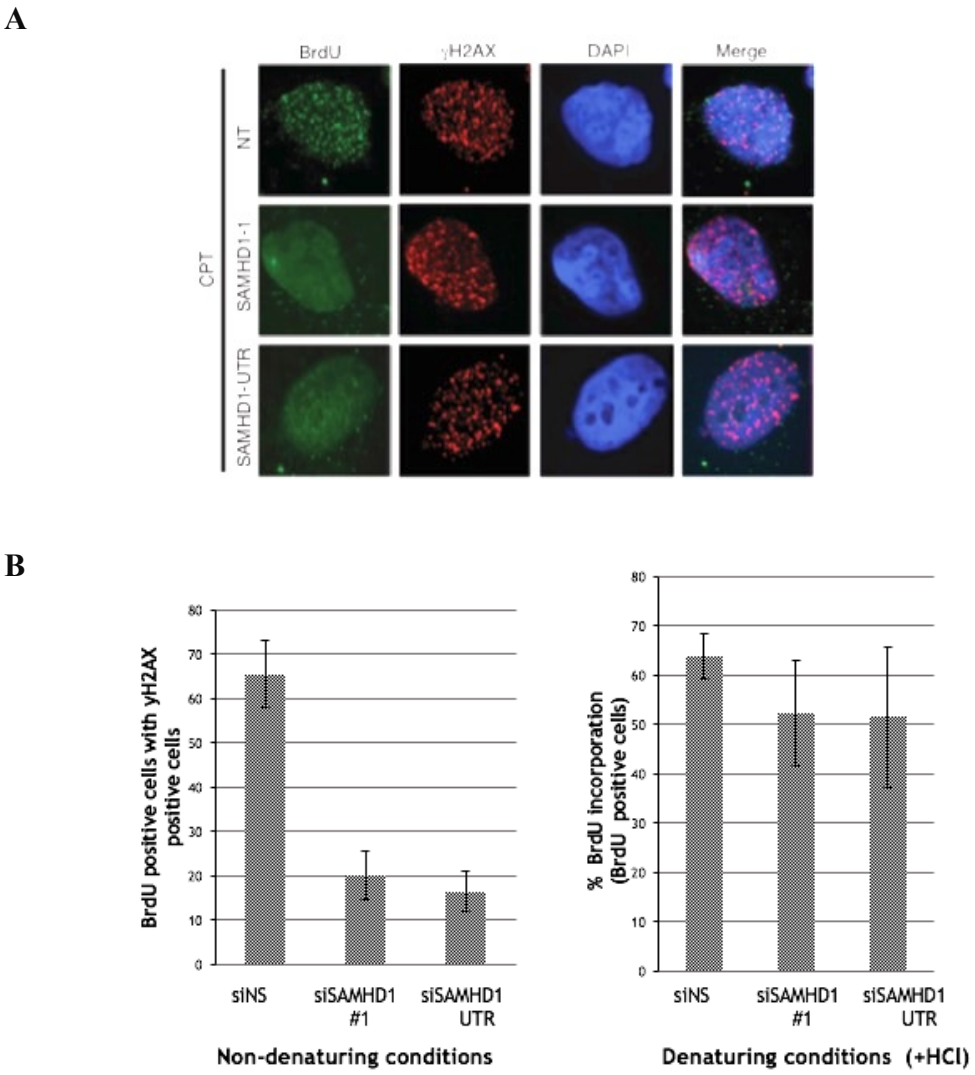

Figure 11*: *SAMHD1 depletion leads to impaired BrdU foci formation. *SAMHD1 knockdown in U20S cells under damage conditions – 3 μM CPT – produces impaired BrdU foci. A) In non-denaturing conditions, siNS maintains BrdU foci formation, whereas siSAMHD1 did not. B) Quantitative analysis of BrdU foci formation in denaturing and non-denaturing conditions.*

Quantification (Figure 11.B) of BrdU foci observed under non-denaturing versus denaturing conditions shows that SAMHD1 knockdown using either of the two siRNAs (siSAMHD1 #1 or siSAMHD1-UTR) impairs RPA70 foci. As a control, staining was also performed following hydrochloric acid (HCl) denaturation, which unwinds the DNA and reveals ssDNA. This control shows that all cells equally incorporated BrdU regardless of the siRNA treatment. Thus, the difference in BrdU foci in non-denatured samples is attributed to reduced resection, rather than diminished BrdU uptake. The above data demonstrate that SAMHD1 is required for efficient end resection, and provides preliminary insight into how to approach SAMHD1's role in homologous recombination.

SAMHD1 knockdown impairs RPA70 foci

SAMHD1's triphosphohydrolase (dNTPase) activity requires binding of dGTP at an allosteric site, which promotes SAMHD1 tetramerization. The residue D137 has been identified as required for dGTP binding [19]. The D137N mutation disrupts dGTP binding, which destabilizes the SAMHD1 tetramer and reduces dNTPase activity. To investigate whether or not SAMHD1's dNTPase activity is relevant to end resection, I tested the ability of SAMHD1 D137N to rescue resection activity in siRNA treated cells.

For these experiments, I used an RPA70 foci assay as a marker for end resection as an alternate to BrdU. An RPA70 foci assay is biologically relevant, since it mirrors the cells' repair pathway. As mentioned in the introduction, RPA70 is a ssDNA binding protein that occupies DNA following resection [24] . Therefore, as a means to study visualize the relevant biological involvement of SAMHD1 in end resection, I pursued an immunofluorescence RPA70 foci rescue assay to confirm its association in end resection within a realistic mechanism in a cell's repair process, and secondly to establish whether or not SAMHD1 is upstream or downstream of RPA70. Figure 12 demonstrates that a knockdown of SAMHD1 impairs RPA70 foci formation and consequently its recruitment to damage sites. To rescue this phenotype, I introduced the mutation D137N and as the image infers the D137N does not rescue RPA70 impairment. Moreover, SAMHD1 knockdown disrupts RPA70 recruitment to damage sites, thus implying that SAMHD1 could act upstream of RPA70.

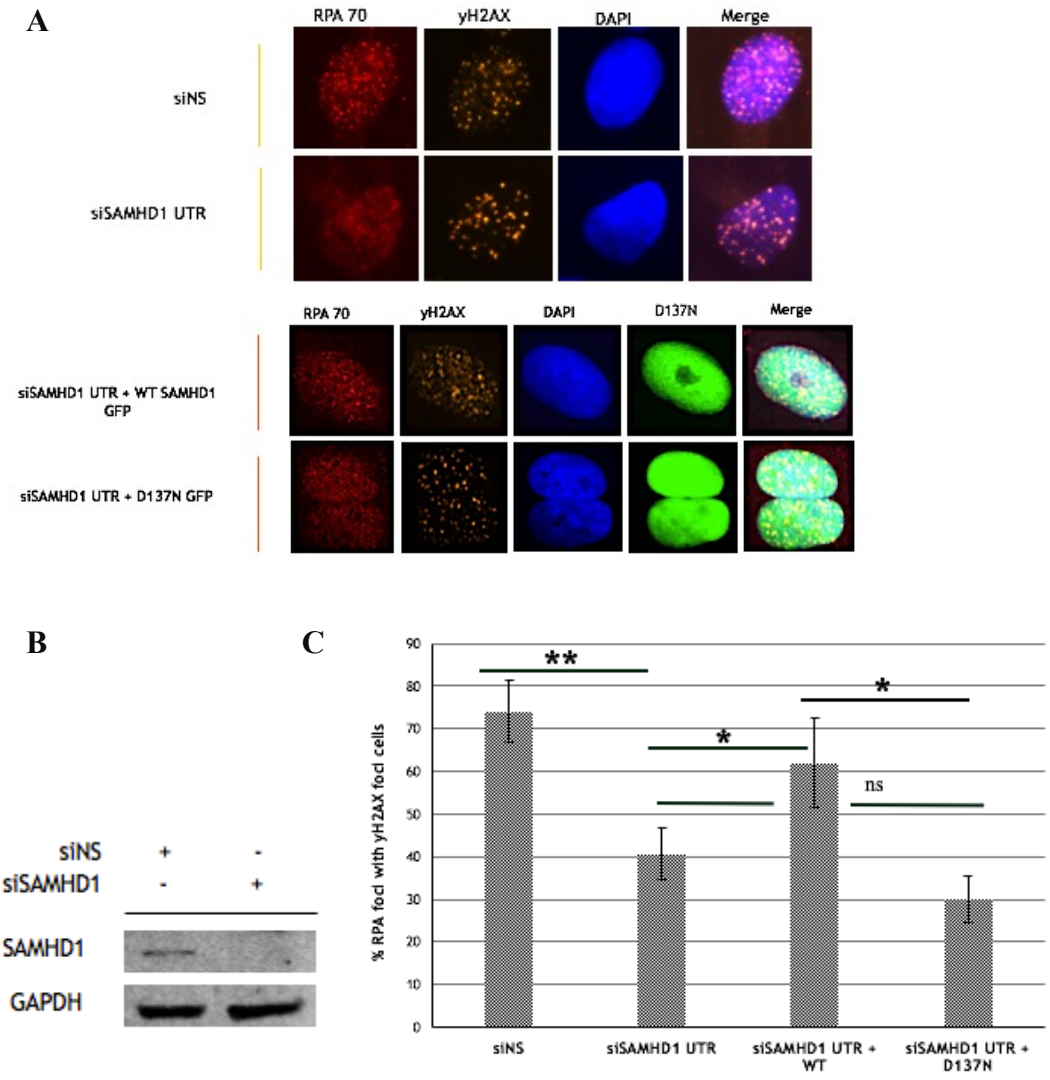

Figure 12: Rescue of RPA70 foci formation following expression of SAMHD1 D137N. *The rescue experiment for siNS and siSAMHD1 UTR U2OS cells were transfected with SAMHD1- GFP D137N plasmid. Following 72 h post knockdown cells were irradiated with 10 Gy and recovered for 4 h. Damaged cells were fixed with 4% PFA (see appendix I. 7) for protocol, and stained with monoclonal anti-RPA70 1:100 and anti- γH2AX-mouse 1:500.A) Visualization of RPA70 foci impairment by siSAMHD1 UTR and siSAMHD1 UTR + D137N, and rescue by wildtype B) Western blot analysis confirms SAMHD1 depletion with siSAMHD1 UTR C) Quantification of the rescue assay, showing significance* (** $P \leq 0.01$, * $P \leq 0.05$, ns $P > 0.05$). *between the impaired foci between siNS and siSAMHD1 UTR. Error bars denote technical replicates of 50 cells in three different fields.*

The quantifications and statistical significance in Figure 12.C confirm that SAMHD1 depletion (shown in Figure 12.B) has impact on end resection efficiency. My controls siNS and siSAMHD1 show a significant difference. The rescue by wildtype also possesses statistical significance between itself and siSAMHD1 UTR $P \leq 0.05$. The phenotype and lack of statistical significance between D137N and siSAMHD1 implies that these phenotypes are comparable. An explanation for this observation, may due to previously established findings about the residue D137. D137 exists at the interface between SAMHD1 dimers, where dGTP binds allosterically in order to promote SAMHD1 tetramerization and its resulting dNTPase activity [19] - if this site were to be mutated, the aforementioned is compromised. Since the D137N mutant interrupts dGTP binding, it has the potential to disrupt SAMHD1's ability to tetramerize, the configuration through which SAMHD1 acts as a dNTPase. As a result, destabilized SAMHD1 may reduce RPA70 recruitment to damage sites and consequently end resection.

Establishing SAMHD1 and CtIP functional interaction

Following the confirmation that SAMHD1 is associated in end resection, it was necessary to explore its interactions with other well established end resection proteins, such as CtIP. Our preliminary data confirms that SAMHD1 interacts with CtIP after damage (Figure 14.A). However, to test if disease relevant SAMHD1 mutations (DRSM) affect SAMHD1's role in end resection, I carried out (co)-immunoprecipitation assays to use truncated SAMHD1 fragments to refine an interacting region with CtIP and screen for mutations that may impair CtIP interaction in an identified region.

The accompanying data presents SAMHD1 truncations (differing by short amino acid sequences : 1-115. 1-165,1-215. 1-315, 1-465 and 1-562) and their interactions with CtIP.

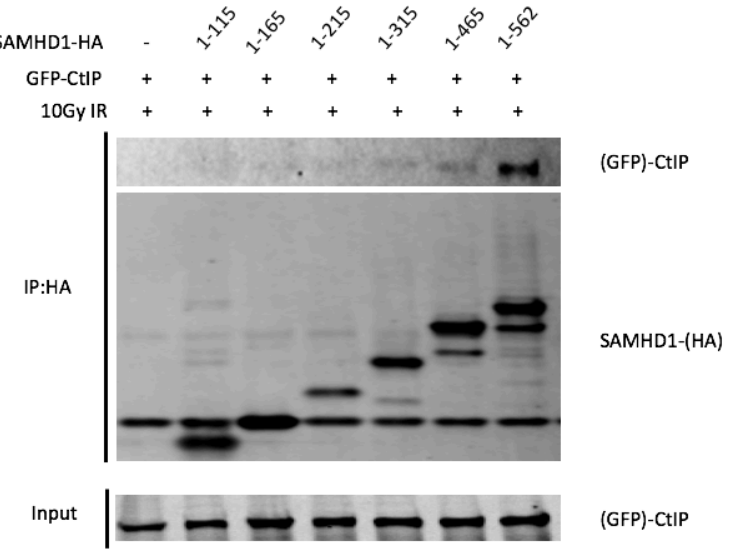

Figure 13: Co-Immunoprecipitation of SAMHD1 CtIP in irradiated cell extracts. *Human 293Ts transfected with SAMHD1-HA truncation expressions: 1-115, 1-165, 1-215, 1-315,1-465, 1-562, and GFP-CtIP. Immunoprecipitation of truncations show pull down GFP-CtIP after irradiation.*

The pull down of CtIP (Figure 13) following SAMHD1 immunoprecipitation suggests that SAMHD1's interacting region with CtIP exists within the region 465-562. There is minimal interaction between truncations ranging below 465. Figure 13 shows that truncation 1-465 and 1-562, have a sudden increase in SAMHD1 and CtIP interaction. We cannot conclude whether or not the interaction between CtIP and SAMHD1 is indirect or direct, but the above data implies that there are critical residues between 465 and 562 necessary for SAMHD1's functional interaction with CtIP. To add to this finding, I intended to identify disease relevant SAMHD1 mutations that possessed the ability to impair SAMHD1's interaction with CtIP.

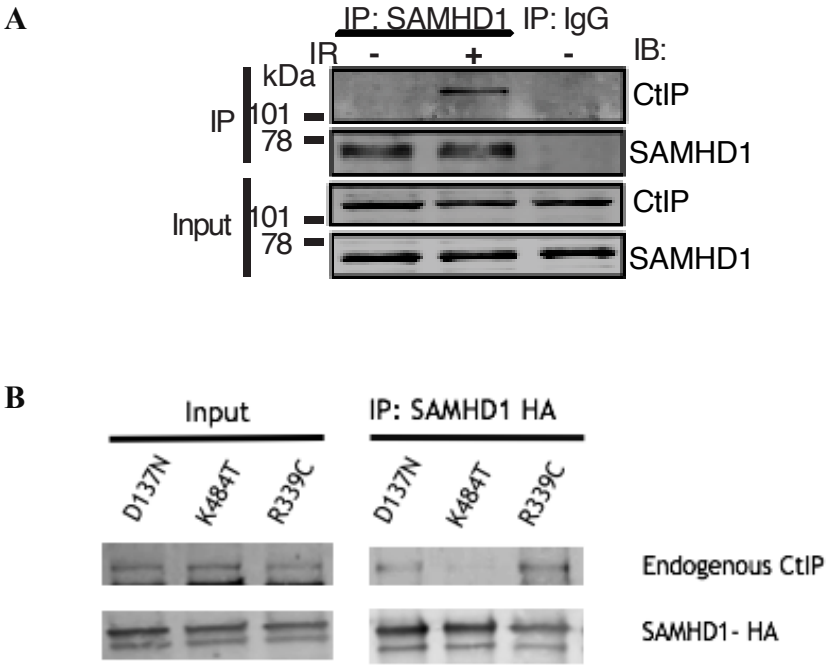

Figure 14: SAMHD1 mutants pull down endogenous CtIP. *Immunoprecipitation of SAMHD1-HA to assess an interaction with endogenous CtIP after irradiation.. A) Irradiation shows SAMHD1 and CtIP interaction is observed. B) Presenting SAMHD1 disease relevant mutations: D137N, K484T and R339C – HA and their respective CtIP interaction.*

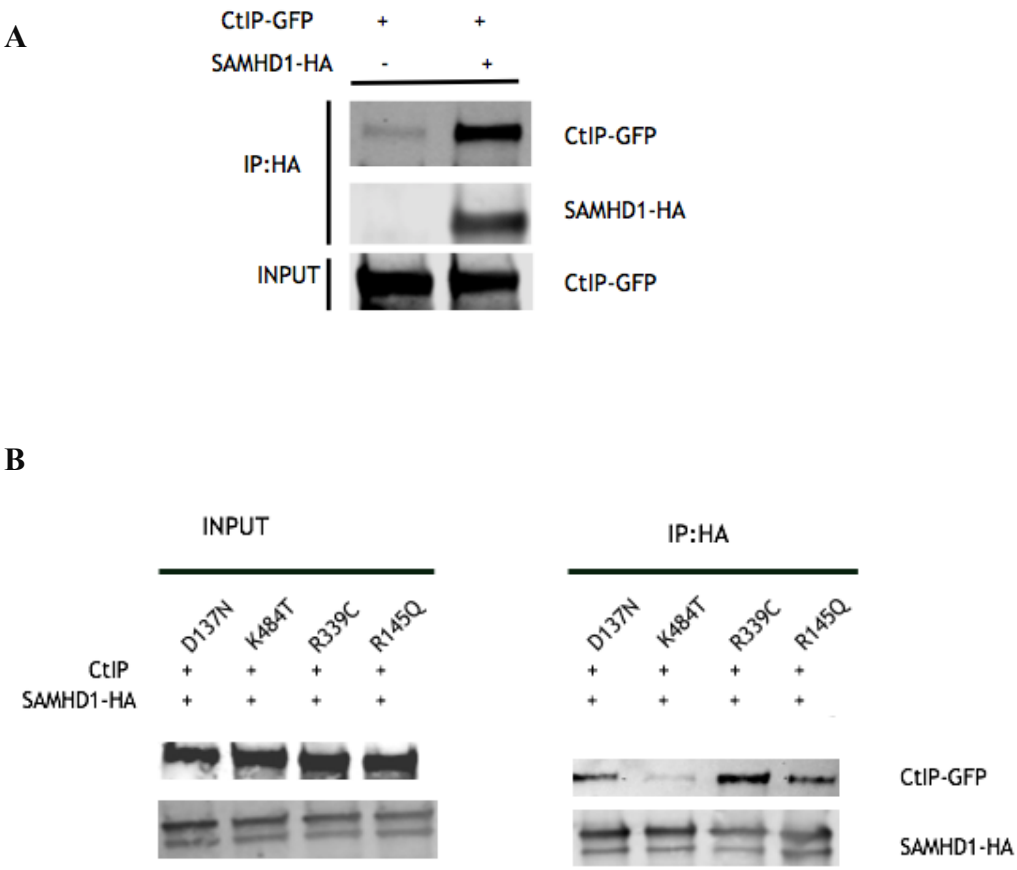

Figure 15: SAMHD1 mutants pull down exogenous CtIP. *Co- Immunoprecipitation isolates the interaction between SAMHD1 and exogenous CtIP after irradiation. A) Co-immunoprecipitation shows SAMHD1 and CtIP interact. B) SAMHD1 disease relevant mutations D137N, R145Q and R339C, serve as confirmation that in comparison to other mutations, K484T shows reduced CtIP interaction.*

Figures 14.A and 15.A serve as are a western analysis of SAMHD1 wildtype confirming an interaction with endogenous and exogenous CtIP respectively. Ideally, I aimed to identify a mutation site within the interacting region 465-562 that impairs SAMHD1 interaction with CtIP. Figures 14.B and 15.B are a preliminary insight into identifying SAMHD1 mutations that impair CtIP interaction. Figure 14.B is a visualization of the expression constructs SAMHD1 D137N, K484T and R339C, and their interaction with endogenous CtIP following irradiation. Figure 15. B is similar to Figure 14.B in that it is a visualization of the expression constructs SAMHD1 D137N, K484T, R339C and R145Q. In both of these panels K484T has the most reduced CtIP interaction in comparison to the other mutations. There are a myriad of reasons to explain this phenotype, so I will expand on these possibilities in my upcoming discussion.

I chose the aforementioned mutations, which have been previously published, to act as controls of each other. R145Q and R339C are mutants located within the HD domain. R145Q was observed in patients diagnosed with AGS and CLL[25]. Therefore, we assume that this overlapping mutant is a link between the two diseases characterized by genomic instability (2). R339C is a residue that appears to have clinical significance, as the site (per a cBioportal analysis) seems to be frequently mutated (there are various forms of mutations at this site) in patients who possess a mutation in SAMHD1 (Figure 7). Both of these mutants and D137N reside around the HD domain (167-311) and appear to show no significant impairment in CtIP interaction, in comparison to K484T.

To follow up with the previously observed phenotypes concerning K484T in Figure 14 and 15., I repeated the Co-Immunoprecipitation in parallel with SAMHD1 WT (Figure 16), to confirm that the mutation suggests an impairment with CtIP.

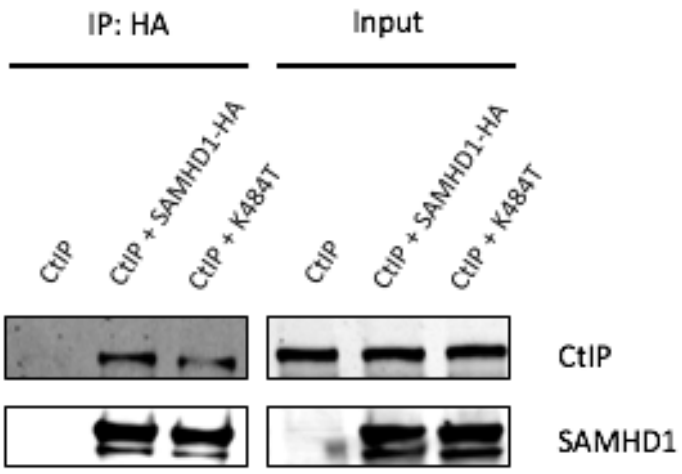

Figure 16: SAMHD1 K484T has reduced CtIP interaction. *Co-Immunoprecipitation between SAMHD1 and CtIP in HEK293Ts confirms the impairment in interaction in the presence of K484T after irradiation. Under damage conditions, CtIP + K484T shows reduced CtIP interaction, in comparison to SAMHD1 WT +CtIP.*

Figure 16 demonstrates a confirmation of the aforementioned phenotype, that the expression of the SAMHD1-HA K484T mutation has reduced CtIP interaction, whereby SAMHD1-HA is immunoprecipitated. The expression control CtIP+SAMHD1-HA wildtype has a strong interaction with CtIP, but we see a partial impairment with the K484T mutation. I will expand on this finding and other suggested theory's in the upcoming discussion.

DISCUSSION

This project served as a preliminary study into how mutations in SAMHD1 observed in disease impose restrictions on SAMHD1's activity in major pathways, namely homologous recombination. The BrdU assay served as a marker for end resection, to confirm that SAMHD1 is involved in end resection. However, as a means to use a biologically relevant assay to determine SAMHD1's role in end resection, I introduced an RPA foci rescue experiment. This assay consisted of comparing phenotypes produced by siNS (ATGAACGTGAATTGCTCAATT) and siSAMHD1 5' UTR

(ACGCAUGCUGAAGCTAAGTAA), and the rescues by expression constructs D137N and WT.

SAMHD1's participation in end resection has yet to be fully established. D137N impairing RPA70 foci formation could be indicative of the natural site D137 being relevant for SAMHD1 to promote end resection by way of RPA70. This phenotype can be explained

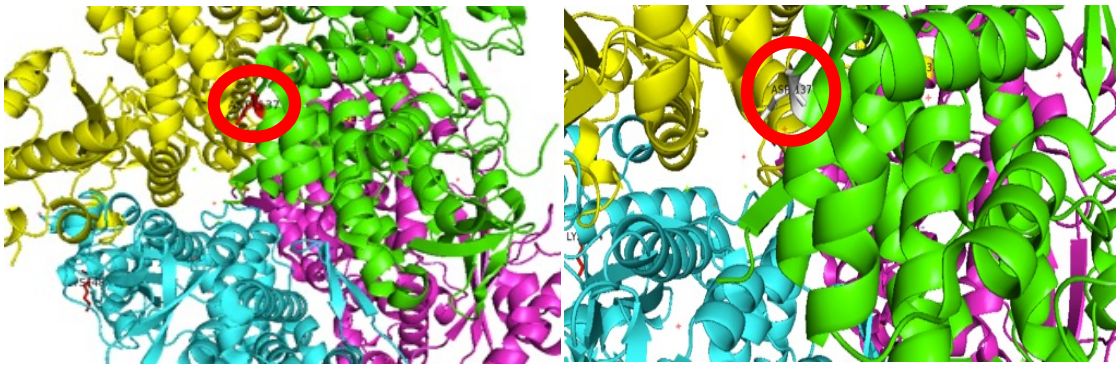

Figure 17: Crystal structure of SAMHD1 tetramer including D137 residue annotated. *Pymol (4BZB) generated crystal structure of SAMHD1 to indicate D137 is located at the interface between dimers [19]*

in a variety of ways, but most interestingly within the context of SAMHD1's structure. In Figure 17 D137 has been previously identified at a dGTP binding site. The allosteric binding of dGTP at four sites, including D137, induces a conformational change which promotes a stable tetramer form of SAMHD1 and yields its catalytic activity [19]

Mutating the amino acid aspartate to an asparagine may result in a variety of consequences on SAMHD1's functionality. Firstly, D137 is located at the interface between dimers thereby suggesting that a mutation to this residue could result in the improper folding of SAMHD1 or unstable tetramer form. The change from aspartate to asparagine (Figure 18) entails a change in charge, particularly from a negative net charge to a neutral.

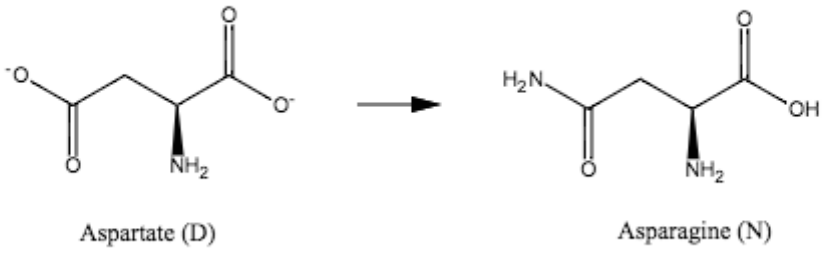

Figure 18: Molecular basis for the change in amino acids, Aspartate to Asparagine.
PerkinElmer Informatics, Chemdraw depiction of Aspartate and Asparagine amino acids.

This change may result in the improper folding of SAMHD1 and the subsequent limited end resection via RPA70 recruitment. Additionally, the interference in dGTP binding may also be due to the change in charge and amino acids. An interruption in

SAMHD1's stable tetramer conformation disrupts its triphosphohydrolase (dNTPase) activity, and thus presumably affects SAMHD1's ability to promote end resection by RPA70 recruitment. However, our previous DR GFP data suggests that HDAA, the catalytically dead mutant (dNTPase deficient), does not impair SAMHD1's participation in HR. In fact, this data proposes that SAMHD1's role in HR is independent of its dNTPase, and that SAMHD1 may possess unknown characteristics that are relevant for HR. This idea would give rise to the possibility that a stable tetramer is significant for SAMHD1 to facilitate HR.

SAMHD1 mutants have the potential to also disrupt SAMHD1's interaction with other proteins, such as CtIP - a major end resection protein. Our co-immunoprecipitation of SAMHD1 truncations imply that the interacting region exists within residues 465-562. Truncations excluding this region presented poor to no interaction with CtIP. To further refine the critical region for CtIP interaction, I screened a set of SAMHD1 mutations to test that a mutation in the 465-562 regions could impair interaction. K484T shows an impairment, whereas mutations R145Q, R339C and D137N do not. In spite of the D137N mutant showing reduced RPA70 (a critical downstream end resection factor) foci formation, it does not appear to affect SAMHD1's association with CtIP. This data would imply that neither the dNTPase nor the stable tetramer is responsible for its upstream role in HR and its association with CtIP.

In comparison to the other mutations I screened for, K484T shows less interaction with endogenous or exogenous CtIP (Figure 14 and 15). To compare with the interaction

with SAMHD1 WT, K484T consistently shows an impairment in CtIP interaction. The cause for the impairment may be similar to D137N, in that the change from a lysine to threonine encompasses a drastic change in amino acid structure (Figure 19) and the subsequent state of the protein.

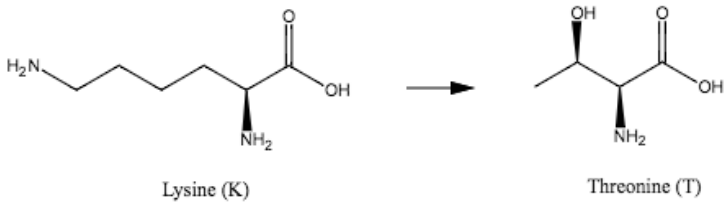

Figure 19: Molecular basis for the change in amino acids, Lysine to Threonine. *PerkinElmer Informatics, Chemdraw depiction of Aspartate and Asparagine amino acids*

Although lysine and threonine carry similar functional groups (carboxyl and amino groups) they vary in their accompanying side chains; lysine has an amino group at the end of its side chain and there is an extra hydroxyl (-OH) group at carbon 3 on threonine. This change in amino acids does not only have the potential to interrupt protein folding, but from a biochemical perspective lysine and threonine are subject to post translational modifications. Lysine's are typically prone to acetylation or ubiquitination, whereas threonine's are likely sites for phosphorylation. Furthermore, the K484 residue is located on the surface of SAMHD1's tetramer, which exposes this site to potential acetyl transferases or any other post-translational modifiers (Figure 20).

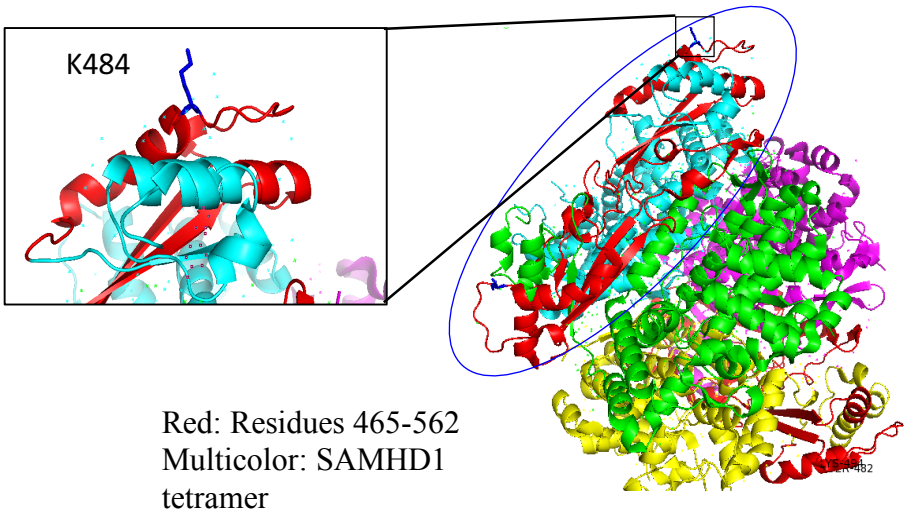

***Figure 20**: **Crystal structure of SAMHD1 tetramer including K484 residue and 465-562 region.** Pymol generated crystal structure of SAMHD1 tetramer, with K484 and 465-562 regions annotated and color coded.*

It is important to note, that it is unclear whether or not the loss of the acetylation site is responsible for promoting the impairment or if it is the gain in potential phosphorylation. There is extensive background on SAMHD1 being regulated by phosphorylation [26], therefore SAMHD1 possessing sites for other forms of post translational modifications could also be considered.

Future Directions

There are several ways to approach this topic. Firstly, to fully characterize the impact D137N and K484T have on SAMHD1 function, it is imperative to test these mutations in the context of standard DNA DSB repair assays – most notably the Direct Repeat GFP (DR GFP) assay to test HR efficiency, and laser micro-irradiation to assess SAMHD1 recruitment to damage sites. According to my previous data, I expect the D137N mutant to reduce HR efficiency, considering that it did not rescue siSAMHD1 UTR impairment of RPA70 foci formation. Similarly, since the K484T mutant impaired CtIP interaction, I would hypothesize that, it too would reduce HR efficiency. Unfortunately, predicting which mutations would impair SAMHD1 recruitment to laser sites of damage would entail identifying key elements responsible for SAMHD1 recruitment. To assess the effect of the mutants, we would need to consider which qualities of SAMHD1 are responsible for its recruitment, including but not limited to: dNTPase, stable tetramer form, monomer/dimer, dGTP binding or even possible nuclease activity. Mutants that have been established (not exclusively D137N or K484T) to either abolish one or multiple of SAMHD1's characteristics will reveal its necessary features for SAMHD1 recruitment to sites of damage, and consequently its potential to promote end resection.

Additionally, I recommend addressing SAMHD1's potential for PTM [27], and the impact it would have on SAMHD1 interacting with other end resection proteins. In the case of K484T, it is imperative to establish whether or not the natural site is post-translationally modified. For instance, it would be beneficial to assess K484's potential as an acetylation

site or as phosphorylation site; we can achieve this by generating acetyl mimics (K484Q), phosphomimics (K484E), and mutants which cannot be modified, acetyl dead (K484R) and phospho-dead (K484A) mutants. If phosphorylation at this residue promotes CtIP interaction, I would expect an increase in CtIP interaction with the phosphomics and a decrease in the phospho-dead, and a similar phenotype to assess acetylation. These modifications contribute to assessing which features of SAMHD1 are responsible for its ability to promote homologous recombination

Although, this study served as a preliminary analysis, there is reason to assume that SAMHD1's mutants [28] could interfere with its activity in end resection - potentially by destabilizing the tetramer, disrupting its dNTPase activity, or adjusting the post translational modification sites. An analysis of SAMHD1's mutants contributes to the overall understanding of SAMHD1's disease relevance, and its role in promoting cancer pathogenesis.

WORKS CITED

1. Saito, Y., H. Fujimoto, and J. Kobayashi, *Role of NBS1 in DNA damage response and its relationship with cancer development.* Translational Cancer Research, 2013. **2**(3): p. 178-189.
2. Panier, S. and S.J. Boulton, *Double-strand break repair: 53BP1 comes into focus.* Nature Reviews Molecular Cell Biology, 2014. **15**(1): p. 7-18.
3. Lu, H., et al., *RECQL4 Promotes DNA End Resection in Repair of DNA Double-Strand Breaks.* Cell Rep, 2016. **16**(1): p. 161-73.
4. Srivastava, M. and S.C. Raghavan, *DNA Double-Strand Break Repair Inhibitors as Cancer Therapeutics.* Chemistry & Biology, 2015. **22**(1): p. 17-29.
5. Yan, J.P., et al., *Tetramerization of SAMHD1 Is Required for Biological Activity and Inhibition of HIV Infection.* Journal of Biological Chemistry, 2013. **288**(15): p. 10406-10417.
6. Zheng, Y.H., K.T. Jeang, and K. Tokunaga, *Host restriction factors in retroviral infection: promises in virus-host interaction.* Retrovirology, 2012. **9**: p. 112.
7. White, T.E., et al., *Contribution of SAM and HD domains to retroviral restriction mediated by human SAMHD1.* Virology, 2013. **436**(1): p. 81-90.
8. Goldstone, D.C., et al., *HIV-1 restriction factor SAMHD1 is a deoxynucleoside triphosphate triphosphohydrolase.* Nature, 2011. **480**(7377): p. 379-82.
9. Beloglazova, N., et al., *Nuclease activity of the human SAMHD1 protein implicated in the Aicardi-Goutieres syndrome and HIV-1 restriction.* J Biol Chem, 2013. **288**(12): p. 8101-10.
10. Ryoo, J., et al., *The ribonuclease activity of SAMHD1 is required for HIV-1 restriction.* Nature Medicine, 2014. **20**(8): p. 936-941.
11. Seamon, K.J., et al., *SAMHD1 is a single-stranded nucleic acid binding protein with no active site-associated nuclease activity.* Nucleic Acids Research, 2015. **43**(13): p. 6486-6499.
12. Wu, L., *SAMHD1: a new contributor to HIV-1 restriction in resting CD4+ T-cells.* Retrovirology, 2012. **9**: p. 88.
13. *United Leukodystrophy Foundation*. Available from: (http://ulf.org/aicardi-goutieres-syndrome.
14. R., W., *Maintaining genome integrity* EMBO Reports, 2006. **7**(4): p. 377-381.
15. Franzolin, E., et al., *The dNTP triphosphohydrolase activity of SAMHD1 contributes to the mitochondrial DNA depletion associated with genetic deficiency of deoxyguanosine kinase.* Journal of Biological Chemistry, 2015.
16. Clifford, R., et al., *SAMHD1 is mutated recurrently in chronic lymphocytic leukemia and is involved in response to DNA damage.* Blood, 2014. **123**(7): p. 1021-1031.
17. Rentoft, M., et al., *Heterozygous colon cancer-associated mutations of SAMHD1 have functional significance.* Proceedings of the National Academy of Sciences of the United States of America, 2016. **113**(17): p. 4723-4728.
18. Uhlen, M., et al., *Proteomics. Tissue-based map of the human proteome.* Science, 2015. **347**(6220): p. 1260419.

19. Ji, X., et al., *Mechanism of allosteric activation of SAMHD1 by dGTP.* Nat Struct Mol Biol, 2013. **20**(11): p. 1304-9.
20. Cribier, A., et al., *Phosphorylation of SAMHD1 by cyclin A2/CDK1 regulates its restriction activity toward HIV-1.* Cell Rep, 2013. **3**(4): p. 1036-43.
21. Bhattacharya, A., et al., *Effects of T592 phosphomimetic mutations on tetramer stability and dNTPase activity of SAMHD1 can not explain the retroviral restriction defect.* Nature: Scientifc Reports, 2016. **6**(31353).
22. SnapGene, *SnapGene® software (from GSL Biotech; available at snapgene.com).*
23. Mattingly, R.R. and I.G. Macara, *Phosphorylation-dependent activation of the Ras-GRF/CDC25Mm exchange factor by muscarinic receptors and G-protein beta gamma subunits.* Nature, 1996. **382**(6588): p. 268-72.
24. Krejci, L., et al., *Homologous recombination and its regulation.* Nucleic Acids Research, 2012. **40**(13): p. 5795-5818.
25. Rice, G.I., et al., *Mutations involved in Aicardi-Goutieres syndrome implicate SAMHD1 as regulator of the innate immune response.* Nature Genetics, 2009. **41**(7): p. 829-U89.
26. Coiras, M., et al., *IL-7 Induces SAMHD1 Phosphorylation in CD4+ T Lymphocytes, Improving Early Steps of HIV-1 Life Cycle.* Cell Rep, 2016. **14**(9): p. 2100-7.
27. Olsen, J.V., et al., *Global, in vivo, and site-specific phosphorylation dynamics in signaling networks.* Cell, 2006. **127**(3): p. 635-48.
28. The UniProt, C., *UniProt: the universal protein knowledgebase.* Nucleic Acids Res, 2017. **45**(D1): p. D158-D169.
29. Wang, W.Y., et al., *Interaction of FUS and HDAC1 regulates DNA damage response and repair in neurons.* Nat Neurosci, 2013. **16**(10): p. 1383-91.
30. Jablonski, L., *Click-iT™ EdU vs. BrdU*. 2007: Invitrogen.

APPENDIX

Appendix I : Protocols

1. DR- GFP assay mechanism diagram:

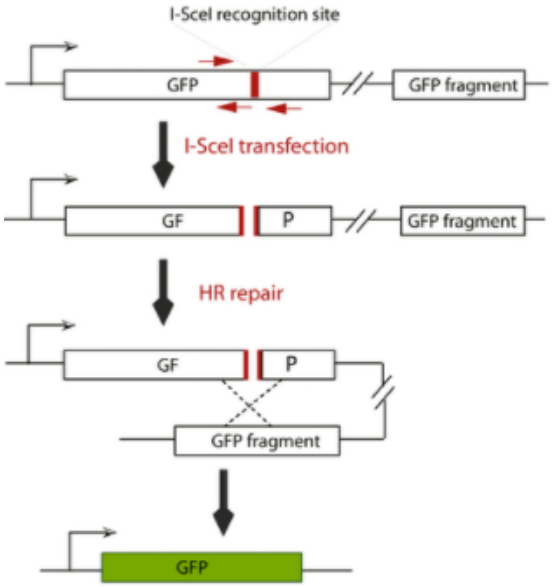

[29]

2. Site Directed Mutagenesis

1 uL of the SAMHD1-GFP plasmid at 50 ng, 1 uL each of the forward and reverse primers at 10 uM, 2 uL DMSO, 1 uL dNTP's, 5 uL of 10X Buffer, 38 uL of ddH_2O and lastly 1uL of Pfu Ultra AD (DNA polymerase)]. Each mutation underwent the following PCR annealing conditions. 50°C (5 cycles) and 60°C (15 cycles). Since the SAMHD1-GFP template was 7.2 kb long, we set each PCR reaction to have an elongation period of 9 min. All PCR products were DpnI digested for 2 h in order to eliminate the potential for any remaining parent DNA, i.e DNA without the desired mutation incorporated. Following this was the expression of all proteins in *Escherichia coli.(E. Coli)* This transformation assay (appendix I.3) was carried out with 20 uL of the cells and 4 uL of the DNA products. Colonies were picked from each transformed plate for a Mini-Prep (appendix I.4). After successful prepping, we validated the mutation via Macrogen sequencing and confirmed using the Snapgene software (appendix I.5).

Method & Reagents

5 µl of 10X Ultra Buffer

1 µl (50 ng) of SAMHD1 - GFP plasmid

1 µl (100 ng) of forward primer

1 µl (100 ng) of reverse primer

1 µl of dNTP mix

2uL of DMSO

38 µl of double-distilled water (ddH2O) to a final volume of 50 µl

Then add 1 µl of DNA polymerase, Pfu Ultra

- Primers generated on Snapgene should have at least 40% GC content, and terminate in either cytosine or guanines.

PCR reaction on PCR program:

1. 95 °C for 2 min - Denature DNA
2. 92 °C for 30 seconds
3. 50 °C 5 cycles and 60 °C 15 cycles
4. 68 °C for 9 min
    a. Repeat steps 2 - 4 for X cycles (desired cycle number)

68 °C for 7 min
Hold at 4 °C (if necessary)

Run gel, the following in their own lanes: 7 uL of 1kb of Ladder, mixture of PCR product (10 uL) and dye (2 uL).

Add 1 uL of DpnI to PCR product and incubate at 37 °C for 2 h, to digest parental DNA. Run 5uL of digested product on a gel and compare to the undigested, there should be a difference in band pattern. Transform into *E. Coli* DH5α

3. Transformation of mutation into DH5-alpha (E.Coli cells)

Method & Reagents

20 uL DH5α

2-4 uL of PCR product

Amp+ plate

- Mix DH5α and PCR product into a 1.5mL microcentrifuge tube, and sit it on ice for 30 min.
- Incubate at 40°C for 30 seconds
- Sit on ice for 2 mins
- Aliquot 980uL SOC into a small falcon tube. Add the entire product in the microcentrifuge tube into the SOC solution. Then shake for 1 h.

Sit the Amp+ plate in room temperature for the time the reagents are in the shaker.

- After an hour, transfer the mixture into a microcentrifuge tube, and spin it down for 3 min.
    - Removed 800 µl out and dispose it.

  Pipette the remaining 200 µl up and down, and plate it onto the Amp+ plate.
    - Use a sterile spreader to thoroughly spread the solution

  Put the plate in the incubator overnight, and count the colonies.

4. Extracting DNA for sequencing – Mini prep Sigma protocol

1.Resuspend the bacterial pellet in 200 µl of the Resuspension Solution.

2. Lyse resuspended cells by adding 200 µl of the lysis solution. Gently invert the tube (6-8 times), until it becomes clear. Do not let reaction exceed 5 min.

3. Add 350 µl of the Neutralization/Binding Solution to precipitate the cell debris. Invert the tube 4–6 times., and centrifuge the cells at ≥12,000 x g or maximum speed for 10 min.

4. Add 500 µl of the Column Preparation Solution to each miniprep column and centrifuge at ≥12,000 x g for 30 seconds, and discard the flow-through liquid.

5. Load the lysate from to the prepared column in step 4. Centrifuge at ≥12,000 x g for 30seconds and discard the flow-through liquid.

6. Wash 1: Add 500 µl of the Wash Solution 1 to the column. Centrifuge at ≥12,000 x g for 30 seconds and discard the flow-through liquid.

7. Wash solution 2: Add 750 µl of Wash Solution 2 to the column. Centrifuge at ≥12,000 x g for 30 seconds and discard the flow-through liquid. Centrifuge the columns again at maximum speed for 1 to 2 min without any additional Wash Solution to remove excess ethanol.

8. Add 50 µL of ddH_2O or molecular biology reagent water to the column. Wait 15 -20 min and centrifuge at ≥12,000 x g for 1 minute.

Nanodrop the product before freezing, to ensure that the DNA concentration is at or above 50 ng/ µL.

5. <u>Preparing the sample for Sequencing</u>

- Mix in blue 500 µL eppendorf tube
- 100ng DNA of interest. (ex. If DNA is at 130 ng/µL 1 µL of the sample is fine)
- 2 µL of 1 µM primer (stock should first be diluted to 1 µM)
- Bring volume up to 15 µL with molecular grade water.

6. <u>Brdu Assay</u>

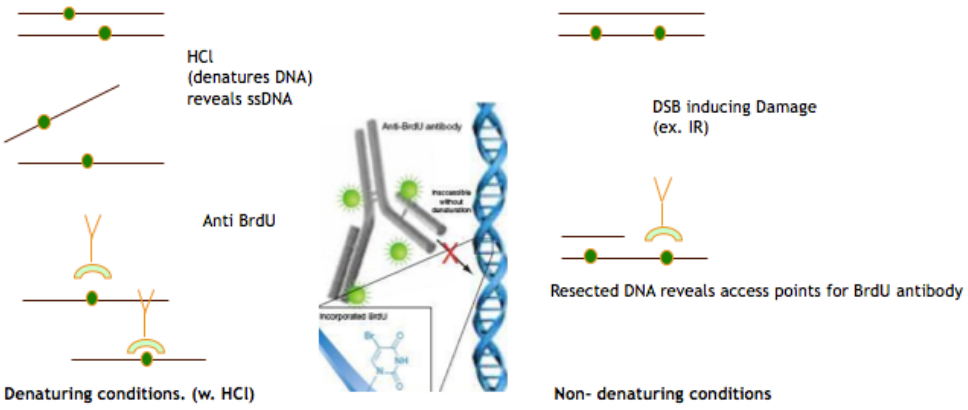

[30]

7. PFA fixation

- Aspirate media
- Wash 1 X 2 mL 1X PBS
- Fix 1mL 4% PFA for 10 min
- Wash 2 X 2 mL 1X PBS
- Permeabilize 1 mL 0.5% Triton X-100/PBS 10 min
- Wash 2X 2 mL 1X PBS
- Block 1 mL 5% BSA/PBS 15 min
- Add 2 M HCl and incubate for 20 min room temperature (pure HCl is 11.6 M)
- Add 0.1 sodium borate, pH 8.5 for 2 min at room temperature
- Wash with 1X PBS for 5 min at room temperature
- Permeabilize 1 mL 0.5% Triton X-100 and 5% BSA in PBS 5 min in room temperature
- Wash 3X with 1X PBS 10 min each wash
- Incubate with anti-BrdU antibody - mouse antibody
- Wash 3X with 1X PBS 10 min each wash

Secondary staining through mounting:

- Wash 4X 2 mL 1X PBS
- Secondary antibody - Alexa 448 - 1:500 in 1% BSA, 0.1% Triton X-100/PBS; 60mcL, 1hours protected from light.
- Wash 4X 2mL 1X PBS, 10 min each wash. Leave final wash over coverslips in well.
- Mount: 3 coverslips/slide, 1 drop (P20 tip) DAP1/coverslips - use scalpel to pry up coverslips

In Situ fixation

- Aspirate media
- Wash 1X 2 mL 1X PBS
- Wash 2X 1 mL CSK buffer
- Pre-extract: 1 mL CSK + 0.5 Triton on rocker for 5 min
- Wash 2X 1 mL CSK buffer, 5 min on rocker
- Fix 1 mL 4% PFA for 15 min.
- Wash 2X 2 mL 1X PBS
- Add 2M HCl and incubate 20 minute room temperature (pure HCl is 11.6M)
- Add 0.1 sodium borate, pH 8.5 for 2 min at room temperature
- Wash PBS for 5 min at room temperature
- 5% BSA in PBS 5 min in room temperature

- Wash 3X with 1X PBS 10 min each wash
- Incubate with anti-BrdU antibody - mouse antibody
- Wash 3X with 1X PBS 10 min each wash
- Incubate 1 h with secondary antibody - Alexa 448
- Wash 3X with 1X PBS 10 min each wash. Add DAP1 in final wash to stain DNA
- Mount slides

Appendix II: Plasmids and Primers

SAMHD1 sequence

MQRADSEQPSKRPRCDDSPRTPSNTPSAEADWSPGLELHPDYKTWGPEQVCSFL
RRGGFEEPVLLKNIRENEITGALLPCLDESRFENLGVSSLGERKKLLSYIQRLVQIH
VDTMKVINDPIHGHIELHPLLVRIIDTPQFQRLRYIKQLGGGYYVFPGASHNRFEH
SLGVGYLAGCLVHALGEKQPELQISERDVLCVQIAGLCHDLGHGPFSHMFDGRFI
PLARPEVKWTHEQGSVMMFEHLINSNGIKPVMEQYGLIPEEDICFIKEQIVGPLES
PVEDSLWPYKGRPENKSFLYEIVSNKRNGIDVDKWDYFARDCHHLGIQNNFDYK
RFIKFARVCEVDNELRICARDKEVGNLYDMFHTRNSLHRRAYQHKVGNIIDTMIT
DAFLKADDYIEITGAGGKKYRISTAIDDMEAYTKLTDNIFLEILYSTDPKLKDARE
ILKQIEYRNLFKYVGETQPTGQIKIKREDYESLPKEVASAKPKVLLDVKLKAEDFI
VDVINMDYGMQEKNPIDHVSFYCKTAPNRAIRITKNQVSQLLPEKFAEQLIRVYC
KKVDRKSLYAARQYFVQWCADRNFTKPQDGDVIAPLITPQKKEWNDSTSVQNP
TRLREASKSRVQLFKDDPM

Primers: blue= mutant amino acids

K484T

Forward: 3’ ggttgccagtgcta**C**acccaaagtattgctag 5’
Reverse: 3’ ctagcaatactttgggt**G**tagcactggcaacc 5’

D137N

Forward: 3’ cctcgtccgaatcatt**AAT**acacctcaatttc 5’
Reverse: 3’ gaaattgaggtgt**ATT**aatgattcggacgagg 5’

R339C

Forward: 3’ ctttattaagtttgcc**T**g**C**gtctgtgaagtagac 5’
Reverse: 3’ gtctacttcacagac**G**c**A**ggcaaacttaataaag 5’

R145Q

Forward: 3’ ctcaatttcaacgtcttc**AG**tacatcaaacagctggg 5’
Reverse: 3’ cccagctgtttgatgta**CT**gaagacgttgaaattgag 5’

pcDNA3-EGFP:

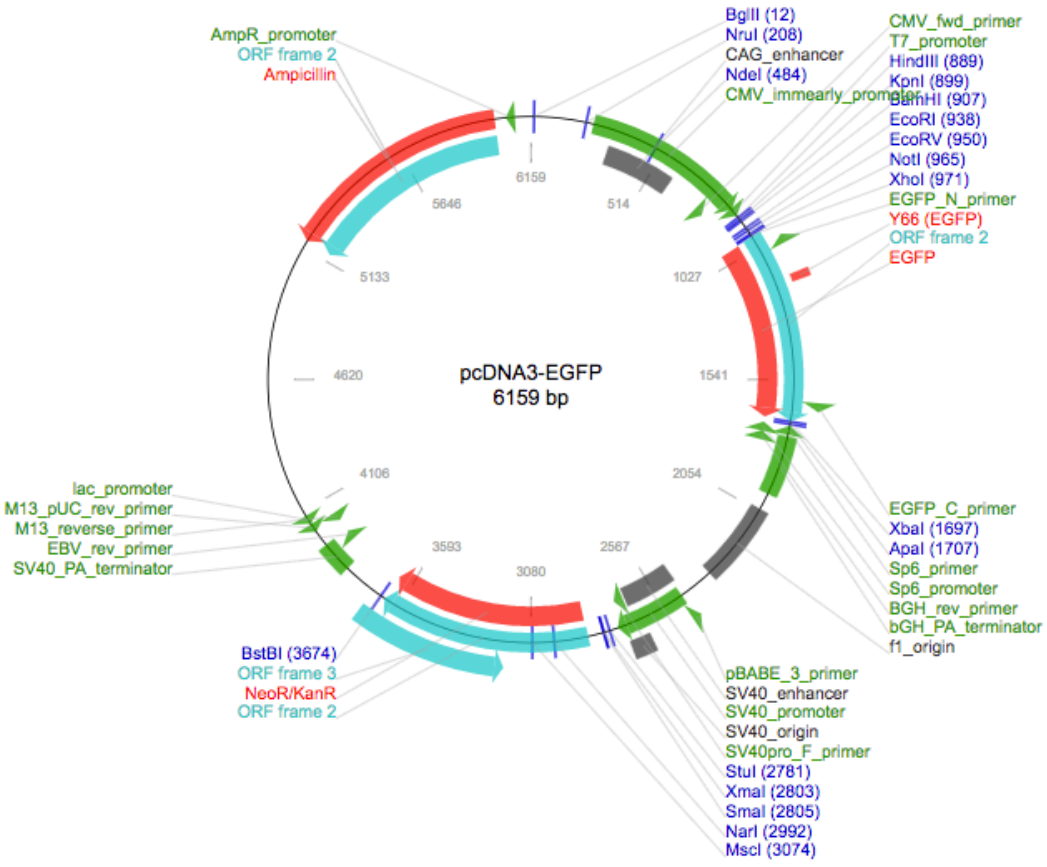
pcDNA3-EGFP
6159 bp
6159
514
1027
1541
2054
2567
3080
3593
4106
4620
5133
5646
AmpR_promoter
ORF frame 2
Ampicillin
BglII (12)
NruI (208)
CAG_enhancer
NdeI (484)
CMV_immearly_promoter
CMV_fwd_primer
T7_promoter
HindIII (889)
KonI (899)
BamHI (907)
EcoRI (938)
EcoRV (950)
NotI (965)
XhoI (971)
EGFP_N_primer
Y66 (EGFP)
ORF frame 2
EGFP
EGFP_C_primer
XbaI (1697)
ApaI (1707)
Sp6_primer
Sp6_promoter
BGH_rev_primer
bGH_PA_terminator
f1_origin
pBABE_3_primer
SV40_enhancer
SV40_promoter
SV40_origin
SV40pro_F_primer
StuI (2781)
XmaI (2803)
SmaI (2805)
NarI (2992)
MscI (3074)
BstBI (3674)
ORF frame 3
NeoR/KanR
ORF frame 2
lac_promoter
M13_pUC_rev_primer
M13_reverse_primer
EBV_rev_primer
SV40_PA_terminator

pKH3:

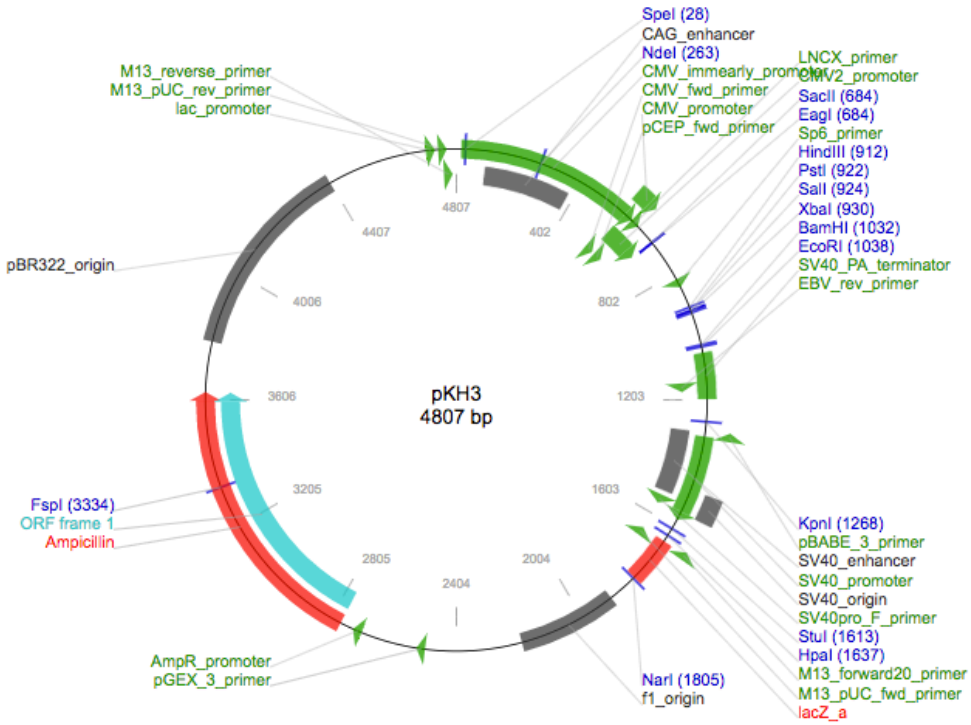
pKH3
4807 bp
SpeI (28)
CAG_enhancer
NdeI (263)
CMV_immearly_promoter
CMV_fwd_primer
CMV_promoter
pCEP_fwd_primer
LNCX_primer
CMV2_promoter
SacII (684)
EagI (684)
Sp6_primer
HindIII (912)
PstI (922)
SalI (924)
XbaI (930)
BamHI (1032)
EcoRI (1038)
SV40_PA_terminator
EBV_rev_primer
KpnI (1268)
pBABE_3_primer
SV40_enhancer
SV40_promoter
SV40_origin
SV40pro_F_primer
StuI (1613)
HpaI (1637)
M13_forward20_primer
M13_pUC_fwd_primer
lacZ_a
NarI (1805)
f1_origin
AmpR_promoter
pGEX_3_primer
FspI (3334)
ORF frame 1
Ampicillin
pBR322_origin
M13_reverse_primer
M13_pUC_rev_primer
lac_promoter
4807
402
802
1203
1603
2004
2404
2805
3205
3606
4006
4407